Downward flame spread and extinction over electric wires placed in a ground-based centrifuge

Yusuke Konno[a,*], Shoryu Ishikawa[a], Nozomu Hashimoto[a], Osamu Fujita[a]

[a] *Hokkaido University, Sapporo, Hokkaido 066-8628, Japan*

Abstract

This study investigates the downward flame spread over laboratory wire samples in a ground-based centrifuge. The specimens consist of low-density polyethylene (LDPE) insulation over metallic cores. Copper (Cu) and nickel-chrome (NiCr) were selected as core materials because they can establish different flame sizes under the same experimental conditions. The centrifugal force is varied from 0 G to 3 G by adjusting the rotational speed of the centrifuge. The flame shapes are photographed from two angles, revealing the tilt of the flame due to the Coriolis force as well as the centrifugal force. Flame spread rates and flame spread limits are also obtained as a function of centrifugal force with oxygen concentration and wire characteristics as experimental variables. As the centrifugal force increases, the flame spread rate decreases and the flammable range narrows. This suggests suppressed flammability under hyper-gravity conditions, explained by finite rate chemistry and thermal effects from flame shape deformation. The Cu sample with large thermal conductivity is strongly affected by the change in heat balance due to the change in flame shape, and the dependence of the flame spread rate and flame spread limit on the centrifugal force is pronounced. Additionally, the displacement of downstream flame is measured with respect to the wire position, and the ratio of Coriolis and centrifugal forces affecting the flame is estimated along with a simple analysis. The ratio of Coriolis force-to-centrifugal force on the flame is found to increase with decreasing the centrifugal force and the radius of rotation decreased.

Keywords: Flame spread; Centrifuge; Gravity effect; Coriolis force; Spacecraft fire safety

---

*Corresponding author.

1) Novelty and Significance Statement

The approach of using a centrifuge to study the impact of gravity on material's flammability is considered novel. Although the idea itself is something that anyone can imagine, few previous studies exist due to complexity of equipment development and phenomena caused by the Coriolis force. Additionally, previous studies are only a couple of decades old, and there are few papers that provide flame images. Therefore, it is valuable to have clear images of how the flame deforms when subjected to centrifugal and Coriolis forces. From a practical point of view, safety issues on the moon and Mars are also a target in the field of manned space exploration, and the demand for scientific experiments and demonstration tests using centrifuges will increase. It is expected that showing how the natural convection induced in a centrifuge is affected by the Coriolis force will provide meaningful knowledge for various scientific experiments, regardless of combustion research.

2) Author Contributions

Yusuke Konn: Writing – original draft; Funding acquisition; Conceptualization; Data curation; Formal analysis

Shoryu Ishikawa: Writing – review; Investigation; Data curation

Nozomu Hashimoto: Project administration; Writing – review & editing; Funding acquisition; Conceptualization

Osamu Fujita: Writing – review & editing

1. Introduction

In the field of combustion research, microgravity experiments have traditionally been conducted using a variety of platforms such as drop towers, airplanes, sounding rockets, space shuttles, and the International Space Station. Meanwhile, centrifuges have been utilized for observing combustion phenomena under hyper-gravity environments [1].

In recent years, there has been a growing research trend, particularly in the space fire safety community, toward the use of centrifuges in microgravity experimental facilities to reproduce partial-gravity environments akin to the lunar and Martian gravity levels [2–4]. This is due to the progress of the U.S.-led Artemis program and the increasing demand to address the new risks and hazards inherent in partial-gravity environments in the realm of human space exploration.

Partial-gravity experiments can be conducted using drop towers and airplanes; however, both approaches have limitations on fall time, posing challenges in achieving experiments for extended durations. Hence, except for direct exploration of the Moon or Mars surfaces, utilizing a centrifuge in the Earth's orbit is the sole viable option for achieving a stable partial gravity for extended periods.

While scientific experiments using centrifuges on the International Space Station have been already carried out in the field of life sciences, there are few instances in the fluid and combustion science that deal with transport phenomena. One significant factor contributing to this is that the generation of artificial gravity through rotational motion also introduces the Coriolis force, adding complexity to the transport phenomena under study. However, there are several previous studies related to combustion experiments that have tackled this complex problem.

Durox et al. [5] have observed both pre-mixed and diffusion flames established over a circular port burner in hyper-gravity conditions realized by a centrifuge. They have reported that when the centrifugal force is applied to a diffusion flame, the downstream tip of the flame is deviated by the Coriolis force. Moreover, they have solved a simplified equation of motion to understand the deflection of the flame due to the Coriolis force and revealed that the deflection of the flame increases as the flame length increases.

Most recently, Lojo et al. [4] have performed numerical simulations to understand the behaviors of the diffusion flame established over a liquid fuel wick placed in a centrifuge. They have found that the flame is significantly deflected by the Coriolis force, resulting in complex circulating flows inside the dome-shaped chamber. Furthermore, they have pointed out that the gravity distribution in the flame becomes non-negligible as the flame size increases.

As stated above, discussing the effects of gravity on combustion phenomena using a centrifuge is not a straightforward problem, yet the demand for experimental systems that can reproduce partial-gravity environments is on the rise. Against this background, this study examined the effectiveness of a centrifuge in evaluating the gravitational effect on the flammability of solid materials. Experimental observations of flame spreading along thin wire samples were carried out under the hyper-gravity conditions on the ground. Although we can only observe the flame spread phenomena in a hyper-gravity environment due to the experiment being conducted on the ground, this study can be valuable for designing centrifuge utilization in microgravity environments, which are anticipated in the future. The dependences of flame spread rates and flame spread limits on the centrifugal force was discussed while observing the flame shape. Furthermore, the contribution of centrifugal and Coriolis forces to the flow field around the flame is examined from the observed flame shapes.

2. Experimental

Figure 1 depicts a ground-based centrifuge designed for this study. The main components are an aluminum frame, motor (BXM6200M-10FR, Oriental Motor Co., Ltd.), slip ring (SRC100-16p, Kyoei Denki Co., Ltd.), and combustion chamber. The inner diameter of the chamber is 390 mm, while the vertical extent within the chamber is 340 mm. The outer

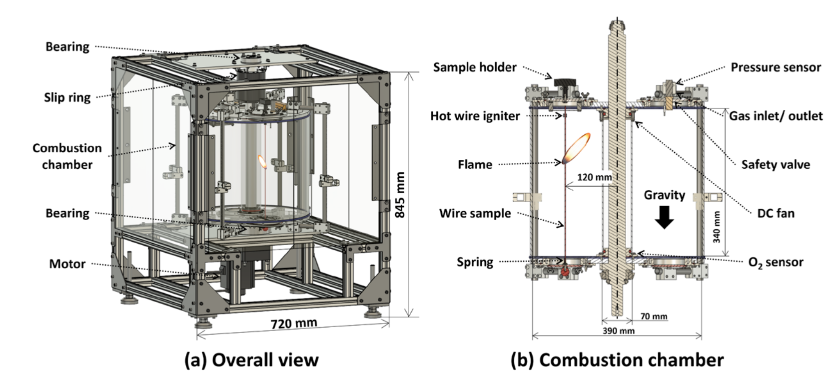

Fig. 1. Schematic of experimental apparatus.

diameter of the rotational shaft spans 70 mm, and the internal volume of chamber approximates 39 L.

Noteworthy is the combustion chamber is hermetically sealed, enabling experimentation under desired atmospheric gases and low-pressure conditions. As illustrated in Fig. 1(b), the specimen was positioned parallel to the rotational axis to ensure a constant centrifugal force acting on the flame as it travels over the specimen. The distance between the rotational axis and the specimen measures 120 mm, and the length of the specimen to be burned is 340 mm. The centrifuge can apply centrifugal forces of up to 10 G (1 G ≈ 9.81 m/s^2) to an object positioned at a radial distance of 120 mm from the rotational axis. In this paper, counterclockwise rotation is defined as positive rotation when viewed from above, unless otherwise noted.

The combustion chamber integrates a pressure sensor (PPX-R01NH-6M-KA, CKD Co., Ltd.), an oxygen partial pressure sensor (JKO-25L3, JIKCO Co., Ltd.), a 3-axis accelerometer (2422-010, Silicon designs Inc.), and two cameras (HERO10 Black, GoPro, Inc.). The time histories of pressure, oxygen partial pressure, and acceleration were recorded on a data logger (midi LOGGER GL240, Graphtec Co., Ltd.) via a slip ring. Additionally, the rotational speed of the motor was recorded on the data logger. The shooting directions of the two cameras are shown in Fig. 2. The image taken from the outside of combustion chamber toward the rotational axis is called as "View A", and the one taken from the right side of View A is called as "View B". As mentioned in previous studies [4–6], flames subjected to the centrifugal force are also affected by the Coriolis force. The influence of each force will be discussed by observing flame images of View A and View B. Note that the GoPro was used in narrow angle mode and the image data used for analysis was corrected for distortion. Furthermore, by photographing the chessboard pattern plates, it was verified that the images were not distorted.

Ignition of the specimen was initiated by an electrically heated wire coil (KAF05, Sakaguchi E.H. VOC CORP.). The power supply to the igniter was regulated by a DC power source (ZX-800, Takasago, LTD). The electric power supplied to the igniter was set to 90 W and the energization time was fixed at 10 seconds. The upper portion of the specimen was ignited and a flame spreading downward along the specimen was observed. In order to start the test with the motion of the chamber and the gas in the chamber matched (the gas in the chamber reaches rigid body rotation), the chamber was rotated steadily for 3 minutes prior to ignition. It is noted that preliminary flow visualization tests using smoke have confirmed that, within the range of the present experimental conditions, the rigid body rotation can be reached in approximately 40 seconds from the start of rotation.

In the present study, laboratory wire samples with an outer diameter of 0.8 mm and a core diameter of 0.5 mm were used, which have been used in our

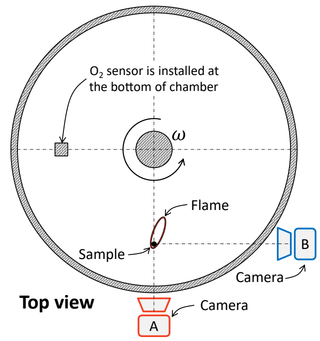

Fig. 2. Position of two cameras and O_2 sensor relative to the sample when observed from the above the apparatus.

previous studies[7,8]. Two kinds of wire samples were tested to investigate the effects of core materials on the flammability of insulation material. Copper (Cu) and nickel-chrome (NiCr) were used for metallic cores, since different flame sizes can be observed under the same experimental condition. Low-density polyethylene (LDPE) was selected as an insulation material. Centrifugal force is varied in the range of 0–3 G. Note that the rate of centrifugal force fluctuation during the experiment was confirmed to be less than 1% by an acceleration sensor in the rotational speed range of the centrifuge used in this study. Mixture of N_2 and O_2 gases was used as oxidizer. The initial total pressure in the chamber was fixed at 100 kPa. The volume fraction of O_2 in the oxidizer was varied in the range of 15–21%.

3. Results and Discussion

3.1. Flame shapes

Figure 3 shows instantaneous flame shapes observed during the downward flame spread under various centrifugal force fields. For each condition, the images of View A and View B described in Fig. 2 are presented and the flames formed along the Cu and NiCr samples are compared.

Because the experiments were conducted on the ground, flames stood vertically in the absence of centrifugal force (Fig. 3(A-Cu0) and (A-Ni0)) and flames formed an axisymmetric candle flame-like shape. However, when the centrifugal force was applied to the flame, the downstream flame tilted and moved away from the bare wire in the burned zone.

A force vector of the buoyancy induced by the centrifugal force is in the radial direction from the specimen position toward the rotational axis. Therefore, the flame tilt angle in the View B increased as the centrifugal force increased. However, as seen in the View A, flames tilted in the circumferential direction as well when they were subjected to centrifugal force.

The observed circumferential tilting of the downstream end of the flame is undoubtedly attributed to the Coriolis force. In the present study, the combustion chamber underwent counterclockwise rotation. Consequently, objects moving perpendicular

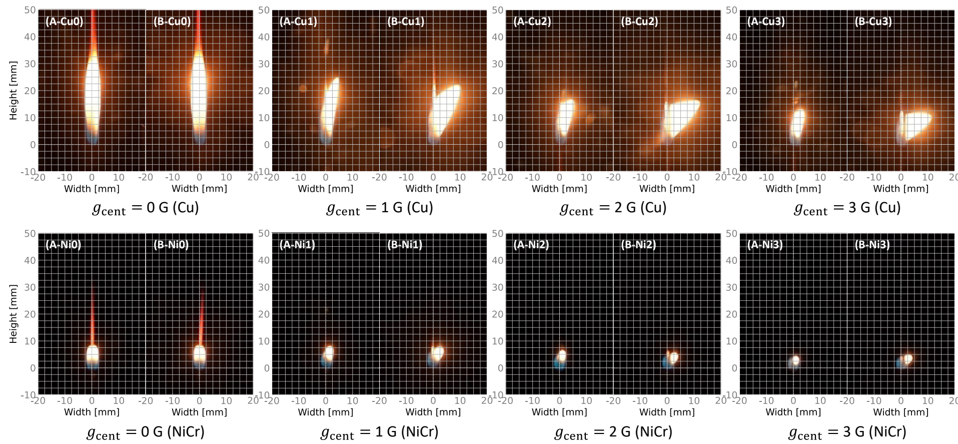

Fig. 3. Instantaneous flame shape observed during flame spread under various centrifugal forces at 21% O_2 concentration.

to the rotational axis in the centrifuge are subjected to the Coriolis force, leading to a consistent deflection to the right relative to their direction of travel. Conversely, under clockwise rotation, the deflection occurs to the left of the direction of travel. Hence, the observed tilting of the flame in both the radial and circumferential directions is a reasonable outcome. Under increased centrifugal force conditions, a segment of the LDPE that melted during flame spread was shaken off from the wire and adhered to the inner wall of the chamber. The trajectory of the molten LDPE was also influenced by the Coriolis force, leading it to adhere to the left side of the View A illustrated in Fig. 2.

With reference to previous studies [4–6], the effect of Coriolis force has been observed regardless of the size of the rotation radius and the type of specimen. Therefore, it is still necessary to understand how the flow field around the flame is modified by Coriolis force in order to discuss the gravitational effect on combustion phenomena using a centrifuge. A further discussion on the flow field around the flame will be given at a later section.

As seen in Fig. 3, a larger flame was formed along the Cu sample than along the NiCr one. This is because the Cu sample has larger flame spread rates than the NiCr one, as described below. It is also evident that regardless of the flame size, the downstream side of the flame was tilted by Coriolis force as well as centrifugal force.

3.2. Time series data during flame spread event

Figure 4 shows the typical time history data measured during flame spread event in a centrifuge. The specimen is the Cu sample. The centrifugal force of 1 G was applied to the wire location (see Fig. 4(a)).

As seen from Fig. 4(b), the pressure in the combustion chamber started to rise immediately after the activation of the igniter and continued to rise until the specimen burned out. As a result, O_2 partial pressure also increased during flame spread. This is

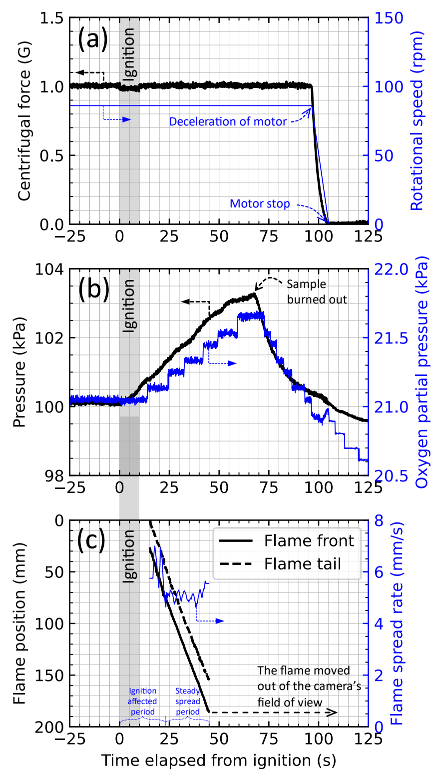

Fig. 4. Typical time series data during the flame spread in a centrifuge. Specimen: LDPE insulated Cu wire, Condition: Centrifugal force = 1 G, Total pressure = 100 kPa, O_2 concentration = 21%. (a) Centrifugal force at r = 120 mm and rotation speed of centrifuge. (b) Total pressure and O_2 partial pressure. (c) Flame positions and instantaneous flame spread rate.

because the rate of increase in pressure was greater than the rate of oxygen consumption and gas mixing in the combustion chamber (note that the O_2 sensor was mounted in the position shown in Fig. 2).

Figure 4(c) shows flame motion history along the wire sample. The leading edge of the upstream flame and the trailing edge of the downstream flame were traced from the visible flame image captured by the camera using in-house python code. The instantaneous flame spread rate was also calculated by applying a Savizky-Golay filter to the flame motion history.

As seen from Fig. 4(c), flame spread process reached nearly steady state after ignition. Therefore, the chamber volume (39 L) can be considered large enough for the specimen to burn, and the effect of time evolution of pressure and O_2 concentration on the flame spread process is negligible. Therefore, the flame front history was approximated as a linear function using the least-squares method, and its slope was defined as the flame spread rate.

3.3. Flame spread rates

Figure 5 shows variations of flame spread rates with centrifugal force. As seen from the figure the Cu sample always showed larger flame spread rate than the NiCr sample in the same experimental condition. This tendency is consistent with previous studies which investigated the effect of core material on flame spread process [7–10]. As repeatedly pointed out in many previous studies, the presence of a metal conductor in a flammable material causes a heat cycle in which the unburned material is heated through the metal conductor heated by the flame. Therefore, a wire sample with a metallic core of larger thermal conductivity has a greater flame spread rate.

Regarding the effect of centrifugal force on flame spread rate, a monotonic decrease was observed with increasing centrifugal force. However, the rate of change in flame spread rate with centrifugal force was more pronounced for the Cu sample than the NiCr one.

In this experimental system, the influence of centrifugal force on the flame spread process can be understood through two factors: alterations in the flow residence time of reactants in the reaction zone and the deformation of the flame shape. Both factors arise from changes in the flow field around the flame. The former is an effect derived from reaction kinetics, wherein the flame temperature decreases with a reduction in the Damköhler number. The latter is a thermal effect involving changes in the heat feedback from the flame to the sample. Observing the trends in flame spread rates shown in Fig. 5 alongside flame shapes presented in Fig. 3 reveals a significant influence of the extent to which the downstream bare wire is enveloped by the flame on the flame spread process along the Cu sample. This observation aligns with findings discussed in the flame spread tests by Hu et al. [10], where the inclination angle of the wire was a variable. Their study revealed that under conditions where the downstream side of the flame envelops the bare wire, the heat conduction through the core to the unburned zone is more substantial, resulting in an increased flame spread rate.

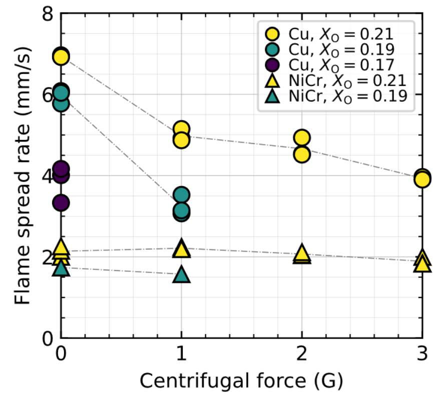

Fig. 5. Flame spread rate as a function of centrifugal force in different O_2 concentrations.

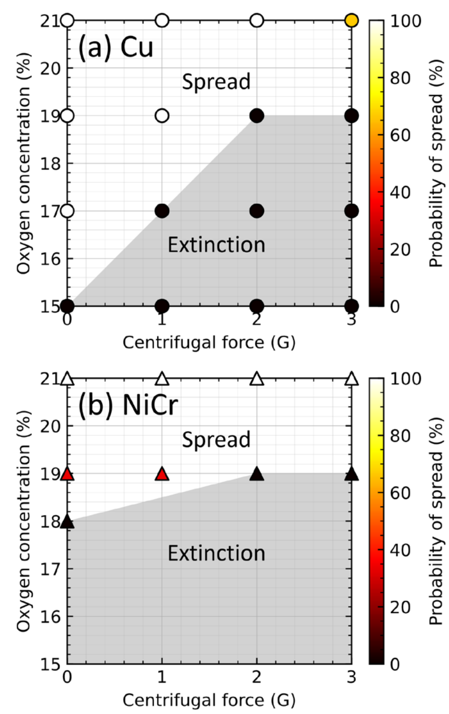

Fig. 6. Flame spread limits as a function of centrifugal force.

3.4. Flame spread limits

Figure 6 shows flammability maps as a function of centrifugal force for Cu and NiCr samples. The experiments were repeated three times under identical conditions, and the likelihood of flame spread or extinction was denoted by the color of the marker (probability of spread was calculated as the number of times the flame spread/number of experiments). White signified consistent flame spread, while black indicated consistent flame extinction.

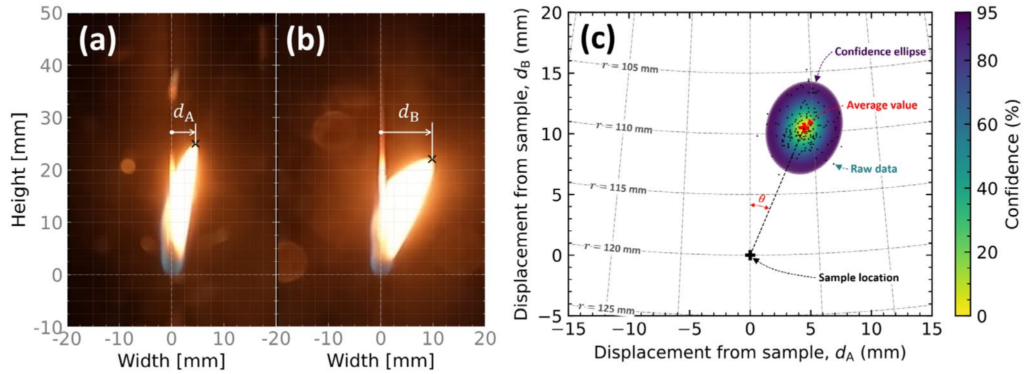

Fig. 7. (a) and (b) show measurement points of downstream end of the luminous flame in View A and B, respectively. (c) shows the how the displacement of the downstream end of the luminous flame is evaluated when the centrifuge is viewed from above. Specimen: LDPE insulated Cu wire, Condition: Centrifugal force = 1 G, Total pressure = 100 kPa, O2 concentration = 21%.

In both samples, the flammable range narrowed as the centrifugal force increased. Moreover, as with the flame spread rate, the Cu sample exhibited a more pronounced rate of change in the flammable range in response to alterations in centrifugal force compared to the NiCr one. These tendencies in the flammable range aligns with the mechanism governing changes in flame spread rate when the centrifugal force varies. Namely, flammability range as a function of centrifugal force is also thought to be influenced by changes in flame temperature due to finite rate chemistry and modifications in heat feedback from the flame due to the deformation of the flame shape. As centrifugal force increases, the natural convection induced by the spreading flame is also enhanced, leading to a decrease in the Damköhler number and a narrowing of the flammable range. Furthermore, as centrifugal force increases and the downstream flame tilts, the flame area enveloping the bare wire on the downstream side becomes smaller, resulting in a lower heat input from the spreading flame to the bare wire and a lower heat input to the unburned insulation.

3.5. Correlation between centrifugal and Coriolis forces affecting the flame

The preceding discussion has highlighted the feasibility of observing the impact of artificial gravity on the flammability of a solid material through the use of a centrifuge. From now on, we attempt to discuss the contribution of both centrifugal and Coriolis forces to the observed flame in the centrifuge.

The shape of the diffusion flame formed along the wire sample can be associated with the trajectory of the gaseous fuel ejected from the wire surface and transported by the surrounding gas flow. Thus, by tracking the downstream end of the flame, the qualitative characteristics of flow field around the flame can be understood.

Figures 7 (a) and (b) show the detection points of a flame tip in View A and View B, respectively. The shortest distance from a flame tip location to a wire

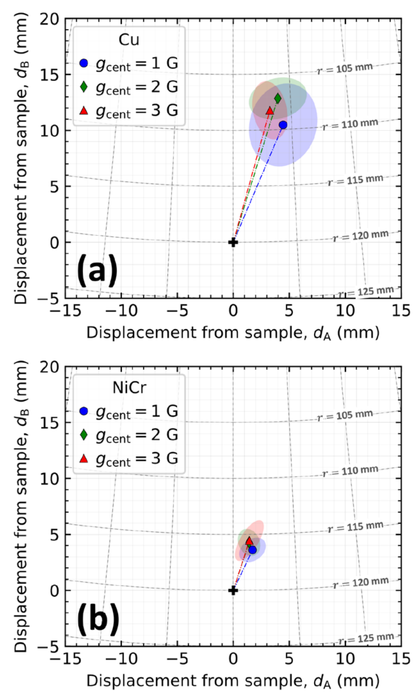

Fig. 8. The position of the downstream end of the flame relative to the wire location. (a) Cu sample, (b) NiCr sample. Initial total pressure = 100 kPa and initial O_2 concentration = 21%.

sample was calculated by considering the distance from a point to a line and the respective displacements were defined as d_A and d_B. Then, using d_A and d_B, plotting the position of the downstream end of the flame relative to the wire location as viewed from the top of the chamber, Fig. 7(c) is obtained. The figure shows the results for the flame spread over the Cu sample under the condition of 1 G of centrifugal force. Since the experiments were repeated three times for each condition, the time histories of each displacement were detected from a total of three movies. The raw data are represented by dots, the average data is represented by a red cross, and the data variability is represented by confidence ellipses. Although the displacement fluctuates a lot due to the flame oscillation during the flame spread process, this method allows us to visualize how much the buoyant flow is deflected by the Coriolis force from a straight line connecting the sample position and the rotational axis. Note that the flame oscillations mentioned earlier are thought to stem from flickering induced by several factors, including the complex circulating flow in the centrifuge, and non-uniformity in the rotational speed of the motor.

The analysis results obtained for the Cu and NiCr samples at centrifugal forces of 1–3 G are summarized in Fig. 8. For simplicity, only the average value and 95% confidence ellipse are presented in the figure. For both the Cu and NiCr samples, the displacement to the right is greater at 1 G compared to the results at 2 G and 3 G.

Here, to quantify the effect of the Coriolis force acting on the flame, the flame tilt angle (θ) relative to the straight line connecting the sample position and the rotational axis was calculated using d_{A} and d_{B} as follows

$$\theta = \tan^{-1}(d_{\mathrm{A}}/d_{\mathrm{B}})\,. \tag{1}$$

Figure 9 shows variations of θ with centrifugal force. θ was calculated for all measurement points of the downstream end of the flame, and the data distributions are presented in violin plots (note that the shaded area in the violin plot shows the probability density of the data on the y-axis). As seen from the data for Cu and NiCr samples, θ increased with decreasing centrifugal force, regardless of the size of the flame. This indicates that as the centrifugal force decreases, the influence of the Coriolis force on the flame becomes relatively more pronounced.

To explain the observed trend in the flame tilt angle shown in Fig. 9, a simple analysis is performed. For the analysis, we first assume that the buoyant flow induced in the radial direction by the centrifugal force is deflected by the Coriolis force, and that d_{A} and d_{B} illustrated in Fig. 7 is caused by the respective forces. Then, the ratio (R_{cori}) of the Coriolis force to the centrifugal force, corresponding to $\tan\theta$ in Eq. (1), is defined as follows

$$R_{\mathrm{cori}} = a_{\mathrm{cori}}/a_{\mathrm{cent}}\,, \tag{2}$$

where

$$a_{\mathrm{cent}} = r\omega^2, \tag{3}$$

$$a_{\mathrm{cori}} = 2\omega u_{\mathrm{cent}}, \tag{4}$$

a_{cent} is centrifugal acceleration, a_{cori} is Coriolis acceleration, r is distance between the sample and the rotational axis, ω is angular velocity, u_{cent} is buoyant flow velocity induced by centrifugal force. u_{cent} in Eq. (4) is defined as an exponential function of a_{cent} as follows

$$u_{\mathrm{cent}} = C a_{\mathrm{cent}}^{n}, \tag{5}$$

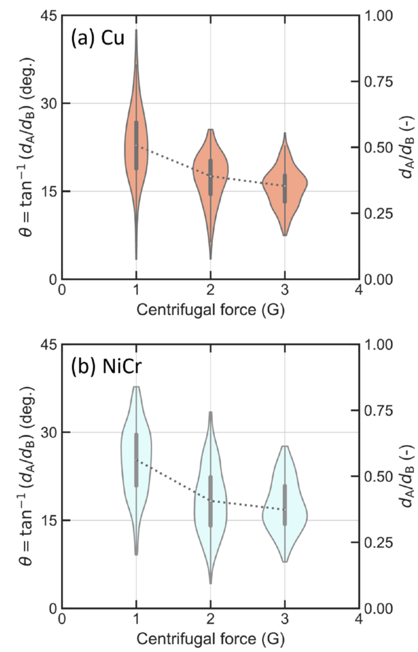

Fig. 9. Relationship between the tilt angle of the flame and the centrifugal force when viewed from the top of the chamber. (a) Cu sample, (b) NiCr sample. Initial total pressure = 100 kPa and initial O_2 concentration = 21%.

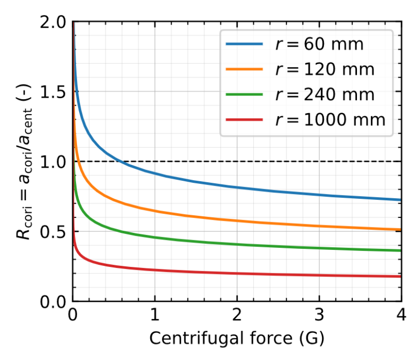

Fig. 10. Variations of relative importance of Coriolis force with centrifugal force.

where C and n are constants. Using Eqs. (2)–(5), we obtain the following equation for R_{cori}

$$R_{\mathrm{cori}} = 2Cr^{n-1}\omega^{2n-1}. \tag{6}$$

The exponent n in Eq. (5) is derived with reference to the analysis of the buoyant flow around the flame induced by gravity [11,12]. Assuming that viscous force is weak and inertial and buoyancy forces are balanced, following equation can be formulated [11,12]

$$u_{\mathrm{cent}}^2/L_{\mathrm{g}} = a_{\mathrm{cent}}\beta\Delta T, \tag{7}$$

where $L_{\mathrm{g}} = \alpha_{\mathrm{g}}/u_{\mathrm{cent}}$ is the thermal diffusion length upstream side of the flame, α_{g} is the thermal diffusivity, β is the thermal expansion coefficient, and ΔT is the temperature difference between flame and surroundings. Rearranging Eq. (7) for u_{cent} yields

$$u_{\mathrm{cent}} = \left(\alpha_{\mathrm{g}} a_{\mathrm{cent}} \beta \Delta T\right)^{1/3} \propto a_{\mathrm{cent}}^{1/3}$$

Thus, n = 1/3 is used for the analysis. The value of C in Eq. (5) was adjusted so that u_{cent} = 35 cm/s at 1 G with reference to previous study [13].

Figure 10 shows the variations of R_{cori} with centrifugal force for r = 60, 120, 240, and 1000 mm. Similar to the trend of the flame tilt angle, the relative magnitude of the Coriolis force increased with decreasing the centrifugal force. However, focusing on the relationship between d_{A} and d_{B} in Fig. 10 and a_{cent} and a_{cori} in Eqs. (3) and (4), it is seen that the changes in d_{A} and d_{B} do not correspond to a change in ω. This is due to the difference in flame length caused by the difference in flame spread rate under each experimental condition. d_{A} and d_{B} are also governed by the amount of fuel. Therefore, it is hereby noted that this analysis can only discuss the relative relationship between the flame displacement due to centrifugal and Coriolis forces, not the absolute amount of flame displacement.

More importantly, as shown in Eq. (6), R_{cori} also depends on the radial distance, and it was found that as r decreases, the effect of the Coriolis force increases even when the same centrifugal force is applied. This result is due to the difference in the dependence of the centrifugal and Coriolis forces on the angular velocity. In several previous studies [14,15] that observed diffusion flame under hyper gravity conditions, it was mentioned that the Coriolis force has little effect on the phenomena, but this may be because R_{cori} becomes smaller under hyper gravity conditions.

As seen in Fig. 10, Coriolis force can exceed centrifugal force when attempting to reproduce the gravity levels of 0.16 G and 0.38 G on the lunar and Martian surfaces using a centrifuge with a small radius of 60 mm. Since this study was conducted on the ground, the natural convection induced in the centrifuge includes a vertical upward component, yet the Coriolis force does not act on an object moving parallel to the rotational axis. This mean that even in a microgravity environment where only the centrifugal force acts on the flame, the correlation between the centrifugal and Coriolis force as shown in Fig. 10 is expected to be observed. Therefore, when using a centrifuge to study the effect of gravity on the flammability of materials, it is desirable to maintain a radius as large as possible and achieve the desired gravity conditions at low rotational speeds. Although this analysis serves only as a rough indication, it agrees with the trend observed in the experiment, and will be a useful guideline when exploring the impact of gravity on combustion phenomena using a centrifuge.

4. Conclusions

The potential of utilizing a centrifuge to explore the impact of gravity on the flammability of thin wire samples was investigated, yielding the following key findings:

- *Flame Appearances*: When centrifugal force is applied to a flame spreading along a wire sample on the ground, Coriolis forces cause the flame to tilt not only radially but also circumferentially.
- *Flammability*: With an increase in centrifugal force, the flame spread rate of the wire sample decreases, and the flammable range becomes narrower. These trends are attributed to two main factors: the effect of the finite rate chemistry due to changes in ambient flow velocity, and the thermal effect arising from alterations in heat feedback from the flame to the wire surface caused by deformation of the flame shape.
- *Material-Specific Trends*: The Cu sample exhibits a more significant rate of change in flame spread rate and flammable range with varying centrifugal force compared to the NiCr one. This distinction is attributed to the high thermal conductivity of the Cu sample, resulting in substantial changes in the amount of heat transported through the wire core when the flame shape is deformed.
- *Flame Tip Displacement*: The displacement of the downstream end of the flame, measured relative to the wire position, reveals an increase in circumferential displacement as the centrifugal force decreases, irrespective of the flame size. This implies that the influence of the Coriolis force on the flame becomes more pronounced relative to the centrifugal force as the latter decreases.
- *Simple Analysis Insight*: An analysis indicates that the dependence of the Coriolis acceleration, acting on the buoyant flow induced by the centrifugal acceleration, and that of the centrifugal acceleration on rotational speed are different. Furthermore, it suggests that the effect of the Coriolis force intensifies as both the rotational speed and radius decrease.

Declaration of competing interest

The authors declare that they have no known competing financial interests or personal relationships that could have appeared to influence the work reported in this paper.

Acknowledgements

This research is supported by JAXA “Kibo” utilization feasibility study, JKA and its promotion funds from KEIRIN RACE, JSPS KAKENHI Grant number JP23K13258, and the Tanikawa-Netsugijyutu Foundation.

Declaration of generative AI and AI-assisted technologies in the writing process

During the preparation of this work the authors used GPT-3.5 and DeepL Translator to enhance the

English language usage. After using this service, the authors reviewed and edited the content as needed and take full responsibility for the content of the publication.

References

[1] Y. Konno, S. Ishikawa, N. Hashimoto, O. Fujita, Evaluation of Buoyant Flow Velocity Induced by Centrifugal and Coriolis Acceleration During Downward Flame Spread Over Thin Wire in a Centrifuge, in: 52nd Int. Conf. Environ. Syst., Calgary Canada, 2023.

[2] P. V. Ferkul, S.L. Olson, Zero-Gravity Centrifuge Used for the Evaluation of Material Flammability in Lunar Gravity, *J. Thermophys. Heat Transf.* 25 (3) (2011) 457–461.

[3] S.L. Olson, P. Ferkul, Evaluating Material Flammability in Microgravity and Martian Gravity Compared to the NASA Standard Normal Gravity Test, in: 42nd Int. Conf. Environ. Syst., San Diego, California, 2012.

[4] A.Z. Lojo, A. Sharma, Y. Liao, M.C. Johnston, P. V. Ferkul, A Numerical Study of Liquid Fuel Wick Flames in Artificial Partial Gravity in a Centrifuge Facility, in: 51st Int. Conf. Environ. Syst., St. Paul, Minnesota, 2022.

[5] D. Durox, T. Yuan, F. Baillot, J.M. Most, Premixed and diffusion flames in a centrifuge, *Combust. Flame*. 102 (4) (1995) 501–511.

[6] M. Arai, K. Amagai, Behavior of a Candle Flame under Super-gravitational Fields, *J. Japan Soc. Microgravity Appl.* 10 (4) (1993) 259–266.

[7] Y. Konno, Y. Li, J.-M. Citerne, G. Legros, A. Guibaud, N. Hashimoto, O. Fujita, Experimental study on downward/opposed flame spread and extinction over electric wires in partial gravity environments, *Proc. Combust. Inst.* 39 (3) (2023) 3785–3794.

[8] Y. Konno, N. Hashimoto, O. Fujita, Downward flame spreading over electric wire under various oxygen concentrations, *Proc. Combust. Inst.* 37 (3) (2019) 3817–3824.

[9] Y. Nakamura, N. Yoshimura, T. Matsumura, H. Ito, O. Fujita, Opposed-wind Effect on Flame Spread of Electric Wire in Sub-atmospheric Pressure, *J. Therm. Sci. Technol.* 3 (3) (2008) 430–441.

[10] L. Hu, Y. Zhang, K. Yoshioka, H. Izumo, O. Fujita, Flame spread over electric wire with high thermal conductivity metal core at different inclinations, *Proc. Combust. Inst.* 35 (3) (2015) 2607–2614.

[11] R.A. Altenkirch, R. Eichhorn, P.C. Shang, Buoyancy effects on flames spreading down thermally thin fuels, *Combust. Flame*. 37 (C) (1980) 71–83.

[12] S. Bhattacharjee, L. Carmignani, Radiation-kinetics interactions: A comparison of opposed-flow flame spread in a low-velocity microgravity and low-pressure downward environments, *Proc. Combust. Inst.* (2020).

[13] S. Takahashi, T. Ebisawa, S. Bhattacharjee, T. Ihara, Simplified model for predicting difference between flammability limits of a thin material in normal gravity and microgravity environments, *Proc. Combust. Inst.* 35 (3) (2015) 2535–2543.

[14] R.A. Altenkirch, R. Eichhorn, N.N. Hsu, A.B. Brancic, N.E. Cevallos, Characteristics of laminar gas jet diffusion flames under the influence of elevated gravity, *Symp. Combust.* 16 (1) (1977) 1165–1174.

[15] H. Sato, K. Amagai, M. Arai, Flickering frequencies of diffusion flames observed under various gravity fields, *Proc. Combust. Inst.* 28 (2) (2000) 1981–1987.